

# Effect of strain and sulfur vacancies on the luminescence and valley polarization properties of CVD grown monolayer MoS<sub>2</sub> films

Poulab Chakrabarti,\* Faiha Mujeeb, and Subhabrata Dhar

*Department of Physics, Indian Institute of Technology Bombay, Mumbai 400076, India*

## Abstract

Using temperature dependent photoluminescence (PL), polarization resolved PL and Raman spectroscopy, we investigate the effect of *in situ* vacuum annealing as well as the relaxation of strain on the luminescence and the valley polarization properties of large area strictly monolayer (1L)-MoS<sub>2</sub>, grown on sapphire and SiO<sub>2</sub>/Si substrates by a microcavity based chemical vapor deposition (CVD) technique. The study shows that the strain as well as the physisorption of air molecules at the sulfur vacancy ( $V_S$ ) sites play key roles in governing the optical quality of CVD grown 1L-MoS<sub>2</sub>. Removal of air molecules from the  $V_S$  sites enhances the relative strength of the A-exciton/trion transition as compared to the broad luminescence (BL) band arising from those defects at low temperatures. It has also been found that such removal helps in improving the valley polarization property of the film. Relaxation of biaxial tensile strain, which has been achieved by post growth transferring of 1L-MoS<sub>2</sub> film from the sapphire to a SiO<sub>2</sub>/Si substrate by a polystyrene assisted transfer process, is also found to be helpful to get back the high polarization character ( $\sim 80\%$ ) of the valleys. The study further shows that the transfer process not only facilitates the removal of physisorbed air molecules from the  $V_S$  sites but also puts in place a long lasting capping layer on MoS<sub>2</sub> that shields the film from reacting with air and hence enhances the relative yield of A-exciton/trion transition by suppressing the BL transition. The study thus creates an opportunity to use CVD grown large area 1L-MoS<sub>2</sub> for the development of optoelectronic as well as valleytronic devices for practical applications for the future.

Single layer (1L) Molybdenum disulfide ( $\text{MoS}_2$ ) has generated significant interest in the last decade due to its novel electronic and optical properties. The material offers several fascinating features, such as direct band gap at the Brillouin zone K-points[1, 2], large exciton binding energy due to reduced dimensionality[3], existence of many body bound states, e.g., trions[4] as well as biexcitons[5] and most importantly spin-valley coupling resulting in valley polarization (VP)[6–8] that can be exploited to inject spin polarized carriers and excitons for future spintronic and valleytronic devices [8–10]. Mechanical exfoliation (ME) and chemical vapor deposition (CVD) are the two most popular techniques to obtain 1L- $\text{MoS}_2$ . However, the two techniques offer contrasting benefits and pitfalls. While, ME can ensure the premium crystal quality of the film by choosing high-grade bulk parent material, getting large area monolayer coverage is impossible in this technique[11, 12]. Whereas, CVD route can synthesize continuous 1L- $\text{MoS}_2$  extending up to a few  $\text{cm}^2$  area[13, 14] providing the necessary platform for the fabrication of large scale integration of devices. Unfortunately however, a large density of sulfur vacancy ( $V_S$ ) related defects[15, 16], grain boundaries[17] and residual strain[18] are invariably present in these films that degrade the device performance. These  $V_S$  related defects, which are known to act as shallow donors in  $\text{MoS}_2$  [19, 20], are shown to be passivated due to physisorption of ambient oxygen-molecules at the vacancy sites leading to the significant reduction of conductivity of 1L- $\text{MoS}_2$  [15, 18, 20]. Photoluminescence (PL) studies on 1L- $\text{MoS}_2$  films often show the presence of a broad luminescence (BL) peak, which is also attributed to the adsorption of ambient oxygen and nitrogen at the  $V_S$ -sites[21]. In fact, there are several experimental studies on the role of surface adsorbates, substrates, strain on the luminescence characteristics of both ME[21–27] and CVD[18, 28–31] grown 1L- $\text{MoS}_2$ . However, very little has been done to experimentally explore the effect of these factors on the valley polarization property of 1L- $\text{MoS}_2$ . These studies are crucial for the development of future valleytronic devices on 1L- $\text{MoS}_2$  platform. Such studies become even more important in case of CVD grown 1L- $\text{MoS}_2$  films as these are always grown on a substrate, which can introduce biaxial strain in the layer and in addition, CVD grown layers possess much higher density of  $V_S$  defects as compared to exfoliated films[16]. Zhu *et al.* have studied the effect of uniaxial tensile strain on the VP properties at room temperature for 1L- $\text{MoS}_2$  obtained by ME technique and found a reduction of VP with the increase of the strain[25]. Saigal *et al.* have reported high value of polarization anisotropy of the A-excitonic PL feature for CVD grown 1L- $\text{MoS}_2$  on  $\text{SiO}_2/\text{Si}$  substrates,

after removing surface residues through high temperature annealing under ultra high vacuum condition[32]. But a systematic effort is needed to understand the underlying mechanism. Moreover, a stable and sustainable method has to be developed to avoid the degradation of the property due to exposure to the ambience. Surrente *et al.* have reported charge transfer mediated VP of 1L-MoSe<sub>2</sub> flakes sandwiched between two more 1L-MoS<sub>2</sub> flakes[16]. However, the maximum degree of circular polarization that they could achieve was only 5%, which is significantly less than the highest value reported in exfoliated samples[6, 7, 33].

Here, we study the effect of systematic *in situ* vacuum annealing and strain relaxation on the luminescence as well as the valley polarization properties of large area strictly 1L-MoS<sub>2</sub> films, grown on sapphire and SiO<sub>2</sub>/Si substrates by a micro-cavity based CVD technique. Investigation using temperature dependent PL, polarization resolved PL and Raman spectroscopy in controlled high vacuum environment, reveals the important roles played by the strain and the  $V_S$  defects that are attached with physisorbed air molecules in shaping the optical properties of the CVD grown 1L-MoS<sub>2</sub>. Removal of air molecules from the  $V_S$  sites has been shown to enhance the relative intensity of the A-exciton/trion feature with respect to the BL band arising from those defects at low temperatures. It has also been observed that the desorption of these molecules from the  $V_S$  defects assists in improving the valley polarization property of the films. As grown 1L-MoS<sub>2</sub> film on sapphire substrate is transferred using a polystyrene (PS) assisted process on to a SiO<sub>2</sub>/Si substrate for investigating the effect of strain relaxation on the optical properties of 1L-MoS<sub>2</sub>. The transfer is found to result in the relaxation of the biaxial tensile strain in the layer, which in turn helps in almost fully recovering the polarization character of the valleys. It has also been observed that the transfer process enables the removal of physisorbed air molecules from the  $V_S$  sites and thus the relative yield of A-exciton/trion transition with respect to the BL band is enhanced. Moreover, the MoS<sub>2</sub> film gets a long lasting PS capping that protects it from the ambient conditions.

Large area monolayer (1L) MoS<sub>2</sub> films were grown on *c*-sapphire (sample P) and  $\sim$ 300 nm SiO<sub>2</sub>/Si (sample Q) substrates by the microcavity based CVD technique, reported earlier by our group[14, 15]. Prior to the growth, substrates were ultrasonically cleaned in trichloroethylene, acetone and methanol successively for 10 minutes each. Sapphire substrate was further cleaned by dipping in a H<sub>2</sub>O:HF (10:1) solution for 40 s. Another sample, ‘P\*’ was prepared by transferring 1L-MoS<sub>2</sub> from the sapphire substrate, where the film was grown

originally, to a SiO<sub>2</sub>/Si wafer. We used a surface-energy assisted transfer method[34, 35], in which polystyrene was first spin coated on the as-grown sample and later baked in two steps; at 80-90 °C for 35 minutes followed by 120 °C for 10 minutes. A water droplet was allowed to get into a gap between the sapphire and the polystyrene coating that results in a gradual removal of the whole polystyrene plus MoS<sub>2</sub> assembly from the sapphire substrate. The assembly was then picked up and placed on top of a SiO<sub>2</sub>/Si substrate before baking it again following the same two step baking recipe. Finally, the sample is dipped in toluene several times to remove the polystyrene coating. More details about the process can be found in the supplementary figure S1. Vacuum ( $\sim 10^{-6}$  mbar) annealing of the samples was performed inside a liquid nitrogen cryostat at 400 K for 30 minutes. Photoluminescence (PL) and Raman measurements were *in situ* carried out on these samples in backscattering configuration at different temperatures inside the same cryostat before and after annealing. A home-built microscope equipped with a 50 $\times$  long working distance objective (NA 0.5) was utilized for these measurements. A 532 nm (2.33 eV) diode pumped solid state laser (DPSS) was used as the excitation source. Signals were recorded by a 0.55 m focal length monochromator attached with a Peltier cooled CCD detector. Polarization resolved PL measurements were also carried out in the same setup, where a linearly polarized 633 nm (1.96 eV) HeNe laser was used as the excitation source. An achromatic quarter waveplate was used to make the excitation left /right circularly polarized ( $\sigma^-/\sigma^+$ ). Another quarter waveplate and a Glan-Taylor analyzer were used to selectively choose left ( $\sigma^-$ ) and right ( $\sigma^+$ ) circularly polarized photons in the collection path of the PL signal (see supplementary Fig. S2). The degree of circular polarization of the collected PL is defined as  $P = (I^+ - I^-)/(I^+ + I^-)$ , where  $I^\pm$  corresponds to the intensity of  $\sigma^\pm$  polarized lights. Intensities of the laser spots on the samples were less than 100  $\mu$ W and 20  $\mu$ W, respectively, for the 532 and 633 nm lasers. Atomic force microscopy (AFM) was carried out at ambient condition on these samples in tapping mode using Bruker, NanoScope-IV system.

Fig. 1(a) compares room temperature micro-Raman spectra for all samples. In all cases, the two characteristic vibration modes, namely the in-plane E<sub>2g</sub><sup>1</sup> and out-of-plane A<sub>1g</sub> features, are clearly evident. Separation ( $\Delta\nu$ ) between the two peaks is found to be  $\sim 20.0$ ,  $20.2$  and  $19.5$  cm<sup>-1</sup> for samples P, Q and P\*, respectively. These values of  $\Delta\nu$  are well within the range for monolayer MoS<sub>2</sub> suggesting that all the samples investigated here are indeed 1L-MoS<sub>2</sub> [14, 15, 36]. It should be noted that the E<sub>2g</sub><sup>1</sup> peak for sample Q (SiO<sub>2</sub>/Si grown)

and P\* (transferred on SiO<sub>2</sub>/Si) appears almost at the same position [ $\sim 383.2 \text{ cm}^{-1}$ ] while, it shows up at  $\sim 384.4 \text{ cm}^{-1}$  for the sapphire grown sample P. This may suggest the existence of more biaxial strain in sample P as compared to other two[13, 15, 18]. A<sub>1g</sub> peak is also down shifted by  $\sim 1.0 \text{ cm}^{-1}$  and  $\sim 1.7 \text{ cm}^{-1}$ , respectively, for sample Q and P\* as compared to that of sample P. This down-shift is likely to be also associated with strain relaxation in the two samples Q and P\*. The reason for some extra amount of shift in sample P\* might be the increase of free electron concentration in the conduction band[37].

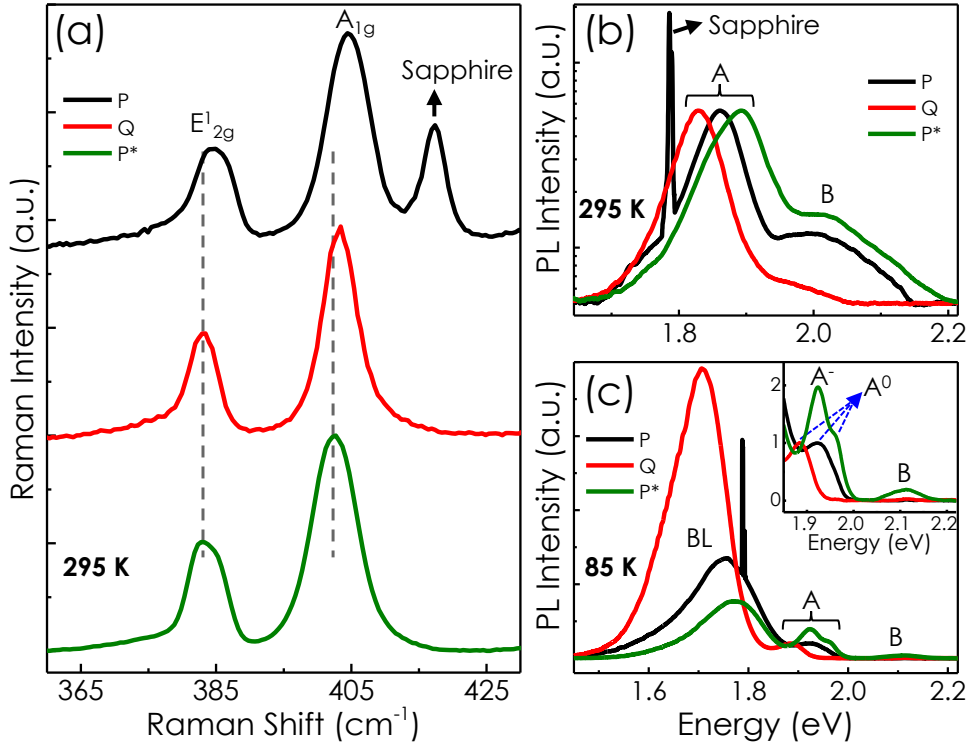


FIG. 1. (a) Room temperature Raman spectra normalized at A<sub>1g</sub> peak for all samples. PL spectra recorded at (b) room temperature and (c) 85 K for all samples. Inset of (c) shows the excitonic transitions in expanded scale. PL spectra are normalized at A exciton (A<sup>0</sup>) peak. 532 nm laser light is used as the excitation source for these measurements.

Fig. 1(b) compares the room temperature normalized PL spectra for these samples, which are featured by two peaks. The most dominant peak appearing at  $\sim 1.86 \text{ eV}$  and a hump at  $\sim 2.0 \text{ eV}$  can be assigned to A and B excitons, respectively. The two excitons result from spin-orbit splitting of the valance band maxima in 1L-MoS<sub>2</sub> [6]. Two sharp spikes at around 1.79 eV for sample P are stemming from sapphire substrate. It should be noted that all

the spectra in panel (b) can be deconvoluted with three Gaussian functions, of which two are needed to fit the A exciton feature. The two can be identified as neutral  $A^0$  exciton and a red shifted charged  $A^-$  trion[4, 6, 15]. It is evident that the A exciton complex is blue shifted (by  $\sim 30$  meV) and broadened for the transferred sample  $P^*$  as compared to the sapphire grown sample P. This suggests a relaxation of a biaxial tensile strain in the  $\text{MoS}_2$  layer after the transfer. It is plausible that such a strain could be developed in 1L- $\text{MoS}_2$  films grown on sapphire substrates due to lattice and/or thermal expansion coefficient mismatch[38–40]. It is well known that biaxial tensile strain can downshift the A excitonic peak position[18, 25, 26]. The increased broadening in the transferred sample can be attributed to the increment in trion weightage as a result of increased electron concentration, which is also consistent with the results of Raman measurements shown in Fig. 1(a). Reason for the enhanced carrier concentration in sample  $P^*$  will be discussed later. Evidently, both the excitonic peaks (A and B-excitons) for the  $\text{SiO}_2/\text{Si}$  grown sample Q are red shifted by  $\sim 30$  meV with respect to those for sample P. Note that the position of  $E_{2g}^1$  Raman peak for sample Q is almost the same as that of the transferred sample  $P^*$  and also matches very well with the reported values for the exfoliated samples[26, 36]. This rules out the presence of strain in sample Q. PL peak shift for this sample thus can not be attributed to strain. This point will be discussed later.

Fig. 1(c) plots 85 K normalized PL spectra for these samples. In addition to band edge A ( $\sim 1.95$  eV) and B ( $\sim 2.1$  eV) excitons, another broad luminescence (BL) feature appears in these spectra at  $\sim 1.75$  eV, which has been attributed to the excitons bound to  $V_S$  defects that are attached with air molecules ( $\text{O}_2$  and/or  $\text{N}_2$ )[21]. Note that the BL feature is earlier been shown to be resulting from excitons bound to S-vacancy related defects in these CVD grown 1L- $\text{MoS}_2$  samples[15, 16]. In another report, it has been further demonstrated that the attachment of oxygen molecules with  $V_S$  defects passivates its shallow donor nature leading to the reduction of the free carrier concentration in these films[20]. Note that in case of the transferred sample  $P^*$ , contributions from  $A^0$  excitons ( $\sim 1.96$  eV) and the trions ( $A^-$  at  $\sim 1.92$  eV)[4, 6] are quite distinguishable from each other as can be seen in the inset of the figure 1(c). This suggests that the density of free electrons in the sample is higher than in two other samples as the trion formation probability is expected to rise with the density of free carriers[3, 6, 18]. This is consistent with the observation of Fig. 1(a). Another interesting point is that the intensity of BL with respect to that of the A excitonic feature

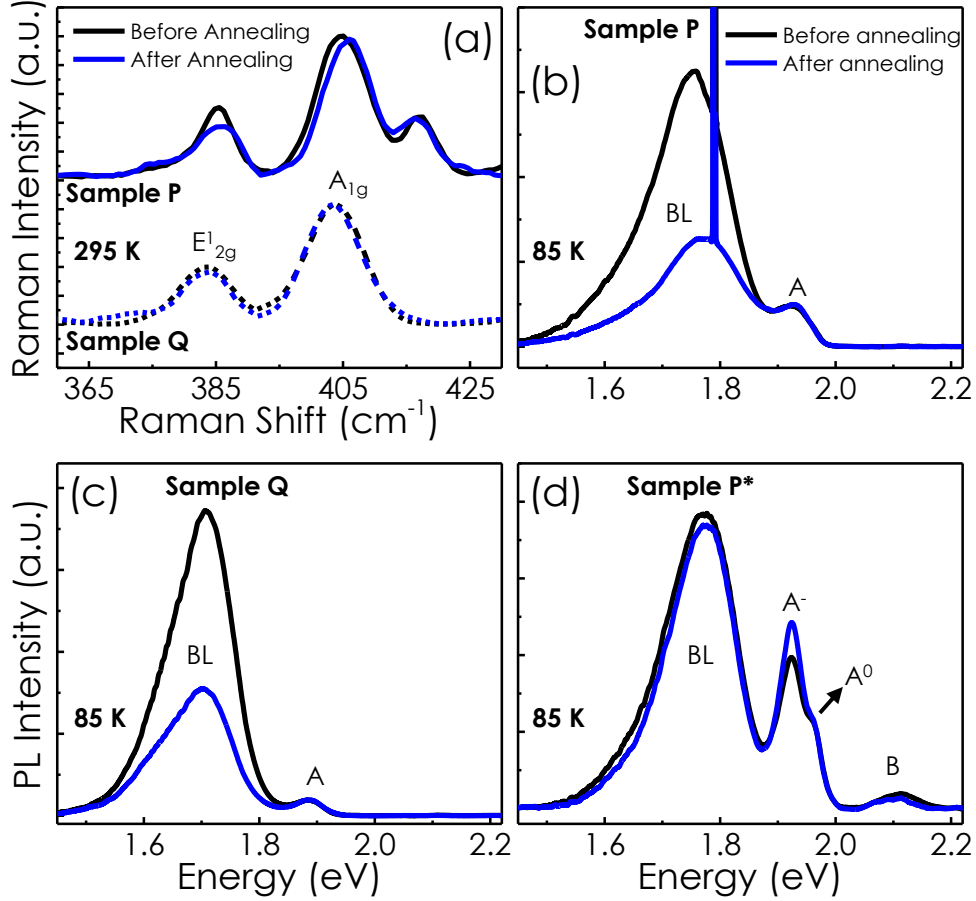


FIG. 2. (a) Room temperature normalized (at  $A_{1g}$  peak) Raman spectra of sample P (solid lines) and sample Q (dashed lines) before (black) and after (blue) annealing. Normalized (w.r.t.  $A^0$  peak) PL spectra recorded at 85 K, before (black) and after (blue) annealing for sample (b) P, (c) Q and (d) P\*. 532 nm laser light is used as the excitation source for these measurements.

is reduced in the transferred MoS<sub>2</sub> film (sample P\*) as compared to the as-grown sample P. This may suggest that the number of attached oxygen molecules (O<sub>2</sub>) with  $V_S$  and hence the passivation of the  $V_S$ -donors has been reduced in sample P\*, which is also in accordance with the observation of enhancement of free electron concentration in the sample with respect to sample P. It should be noted that the BL to A-exciton intensity ratio is the maximum for SiO<sub>2</sub>/Si grown sample Q indicating higher density of passivated S-vacancies. It is plausible that the reduced density of free electrons in this sample can result in the suppression of screening of the electron-hole coulomb interaction potential leading to an enhancement in the binding energy of excitons[24]. This can explain red-shift of all PL peaks in this sample.

Fig. 2(a) compares room temperature Raman spectra for sapphire grown samples P and SiO<sub>2</sub>/Si grown sample Q before and after annealing. It can be seen that for both the samples, Raman peaks before and after annealing overlap with one another which indicates that annealing at 400 K hardly changes the strain state of the materials. Panel (b), (c) and (d) plot normalized (w.r.t. A<sup>0</sup> peak) PL spectra at 85 K before and after annealing for samples P, Q and P\*, respectively. Note that for the as-grown samples P and Q the intensity of the BL feature substantially reduces after annealing. This can be attributed to the desorption of ambient O<sub>2</sub> and/or N<sub>2</sub> molecules from V<sub>S</sub> sites[21]. However, for the transferred sample P\*, where BL intensity is already quite reduced, there is not much of change in BL intensity upon annealing. This result may indicate that most of the S-vacancies are already depleted in this sample. It should also be noted that in sample P\*, there is a slight tendency of increment of relative intensity of A<sup>-</sup> peak with respect to that of A<sup>0</sup> upon annealing. As mentioned earlier that in one of our recent publications, physisorption of oxygen molecules at V<sub>S</sub>-sites is shown to be responsible for the passivation of the V<sub>S</sub> donors leading to the reduction of the free carrier concentration in these films[20]. Observation of annealing driven increase of trion intensity in sample P\* could thus mean that some of the left-over oxygen molecules (O<sub>2</sub>) from the V<sub>S</sub>-sites are removed after annealing leading to the enhancement of density of free electrons in the layer. However the number of such removals is not enough for giving rise to any significant change in BL intensity.

Fig. 3(a) and (b) show circular polarization resolved PL spectra recorded at 85 K temperature for sapphire grown sample P before and after annealing, respectively, where left circularly polarized ( $\sigma^-$ ) 633 nm laser (1.96 eV) is used for excitation. Evidently,  $\sigma^-$  and  $\sigma^+$  polarized PL spectra are overlapping with one another before and after annealing. Fig. 3(c) and (d) show polarization resolved PL spectra obtained with  $\sigma^-$  polarized 633 nm laser excitation at 130 K temperature for sample Q before and after annealing, respectively. While there is no change between the spectra recorded for different polarizations for the sample before annealing, a clear difference emerges at the A-exciton/trion feature after annealing. Inset of Fig. 3(d) plots absolute value of degree of circular polarisation ( $|P|$ ) as a function of photon energy. It is noteworthy that as high as 25% polarization can be achieved at the peak position of A<sup>0</sup>. It should be noted that we have performed the same experiments at 85 K on sample Q before and after the annealing. However, at that measurement temperature, A-exciton/trion feature could not be seen and the BL feature that dominates the



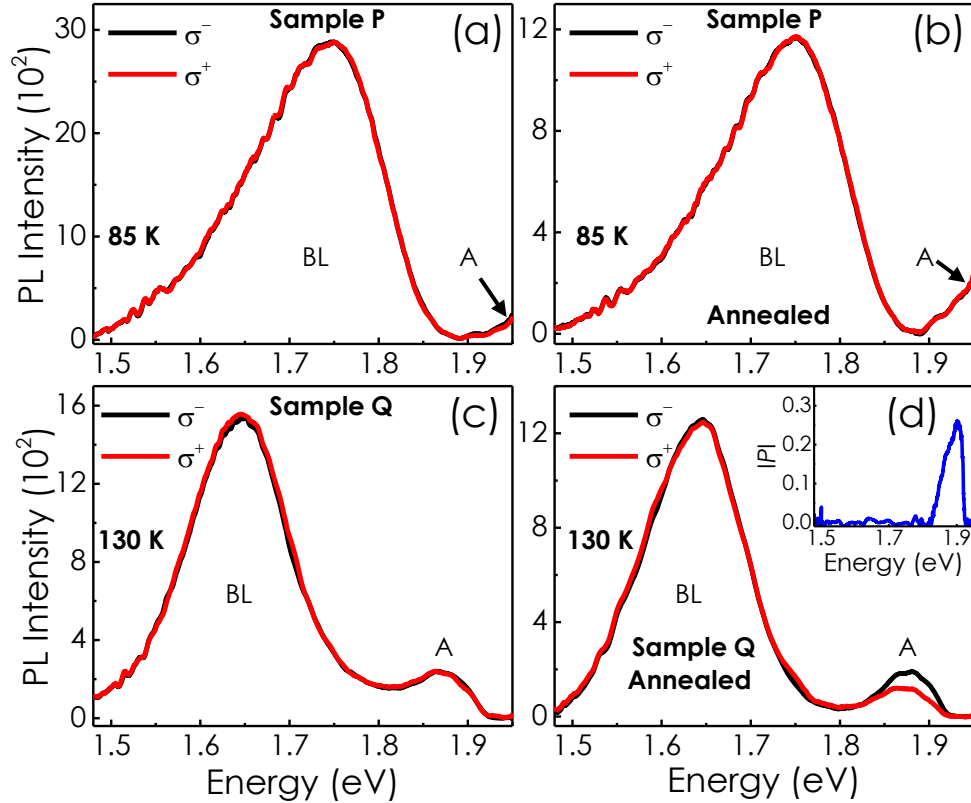


FIG. 3. Circular polarization resolved PL spectra for sample P recorded at 85 K (a) before and (b) after annealing. Same PL spectra for sample Q recorded at 130 K (c) before and (d) after annealing. Inset of (d) shows degree of circular polarization ( $|P|$ ) as a function of photon energy. Black (red) spectra in all panels are obtained for  $\sigma^-$  ( $\sigma^+$ ) polarized luminescence when  $\sigma^-$  polarized light of 633 nm laser is used for excitation.

spectrum is found to be unpolarized both before and after the annealing(see supplementary Fig. S3). At this low temperature, exciton capture rate at the  $V_S$  cites must be much higher than the recombination rate of the free excitons as the energy and power of the 633 nm laser is relatively low[21]. BL feature, which are likely to be originating from the excitons trapped in  $V_S$ -plus-ambient-molecule complexes, has not been reported to show polarization in 1L-MoS<sub>2</sub> [6, 33]. Excitons trapped in these defects are expected to have a spread in their crystal momentum, which can facilitate spin flip scattering between K and K' valleys through Bir-Aranov-Pikus electron-hole exchange mechanism resulting in a mix-up of excitons with opposite spins[6, 41].

Fig. 4(a) and (b) compare  $\sigma^-$  and  $\sigma^+$  polarized PL spectra recorded at 295 K and 85 K,

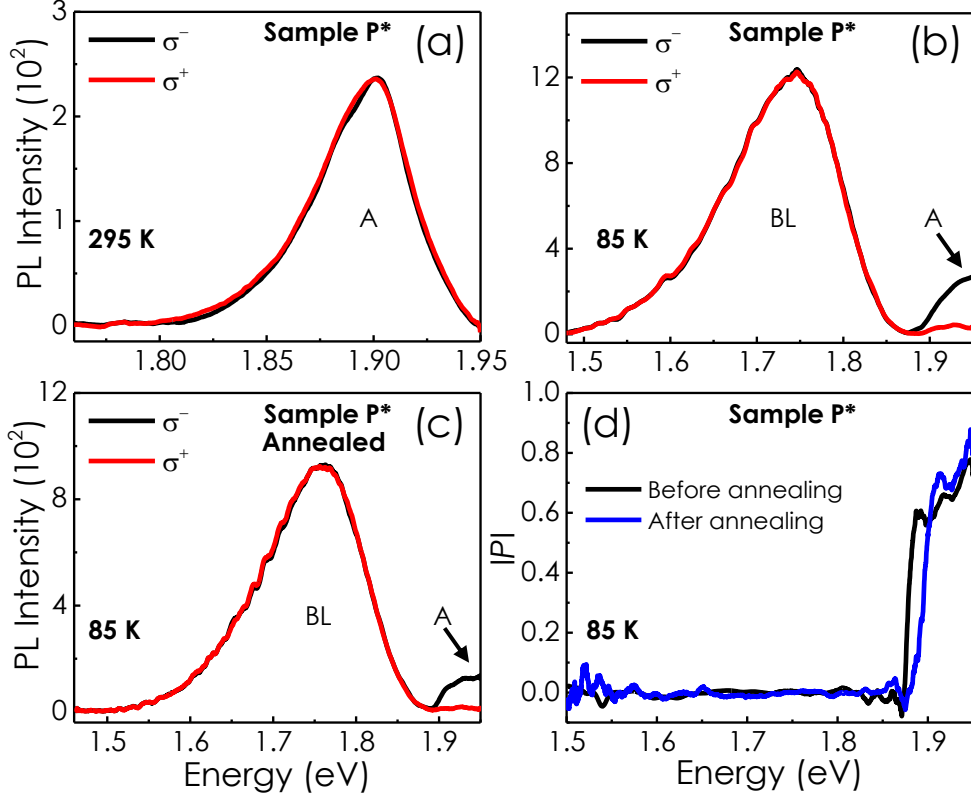


FIG. 4. Circular polarization resolved PL spectra for the transferred sample P\* recorded at (a) 295 K, (b) 85 K before annealing and (c) 85 K after annealing.  $\sigma^-$  polarised 633 nm laser light is used as the excitation source. (d) Degree of circular polarization ( $|P|$ ) as a function of photon energy before (black) and after (blue) annealing.

respectively, for the transferred sample P\*. While at 295 K,  $\sigma^-$  and  $\sigma^+$  profiles overlap with one another, a gap clearly opens up at A-exciton/trion feature at 85 K. Note that gap opening could not be found at the BL feature. Panel (c) shows the comparison between  $\sigma^-$  and  $\sigma^+$  polarized PL spectra for the sample P\* after annealing. It is noticeable that the gap opening at the A-exciton/trion feature is still intact even after the annealing. Fig. 4(d) plots the degree of circular polarization ( $|P|$ ) as a function of photon energy for the sample before and after the annealing. It is remarkable to see that for both the cases,  $|P|$  reaches up to  $\sim 0.8$  at the A<sup>0</sup> exciton position.

Note that in these experiments, layers are excited with a circularly polarized laser light whose energy is in resonance with A exciton complex at 85 K temperature. One should thus expect  $\sim 100\%$  PL-polarization at A-exciton/trion feature in case of an ideal 1L-MoS<sub>2</sub> as K and K' valleys can only accommodate excitons with pseudospin +1 and -1,

respectively[42].  $|P| < 1$  at A-exciton/trion feature should thus mean a deviation from ideality. It is conceivable that the presence of strain and defects in the layer can influence the value of  $|P|$  by introducing spin-flip channels through band structural modification [8, 25, 32]. In fact, it has been experimentally shown that the enhancement of the uniaxial tensile strain can lead to the reduction of  $P$  in exfoliated MoS<sub>2</sub> monolayers[25]. Theory predicts that the increase of uniaxial[25, 26] as well as biaxial[43] tensile strain, leads to the up shift of the energy of the spin degenerate local valance band maximum (VBM) at the  $\Gamma$  point ( $\Gamma_v$ ) in 1L-MoS<sub>2</sub>. Beyond a threshold value of strain, the  $\Gamma_v$ -maximum moves above the VBM at K(K') and the band gap becomes indirect. This tensile strain driven upward movement of VBM at the  $\Gamma$ -point increases the probability of spin flipping via spin-degenerate  $\Gamma$  valley[5, 25]. This is one of the reasons for valley depolarization of 1L-MoS<sub>2</sub>. Here, the sapphire grown sample P has been found to posses the highest amount of tensile strain. Observation of zero PL-polarization in sample P both before and after annealing can thus primarily be attributed to the strain. The findings of Fig. 1 clearly suggest the release of tensile biaxial strain in transferred sample P\*. Relaxation of strain might thus be a reason for the recovery of the polarization in the transferred film. Note that tensile biaxial strain in SiO<sub>2</sub>/Si grown sample Q is much lower than that of the sapphire grown sample P [see Fig. 1]. So, the observation of zero PL-polarization in sample Q before annealing cannot be attributed to the modification of band structure due to strain. Note that the density of S-vacancy defects and hence of  $V_S$ -plus-air-molecule complexes is found to be more in sample Q than in other samples [see Fig. 1(c)] before annealing. Upon annealing, when air molecules are removed from  $V_S$  sites, the intensity of BL feature decreases and at the same time sample Q starts showing a finite  $|P|$  at the A-exciton/trion feature. This suggests that air molecules adsorbed at the  $V_S$  sites might be responsible for nullifying  $|P|$  in this sample. Among different elements in air, O<sub>2</sub> possesses a magnetic moment of 2.0  $\mu_B$  per molecule[44]. One can thus expect the existence of a finite magnetic moment also at the  $V_S$ -plus-O<sub>2</sub>-molecule defect sites. For an example, density functional theory (DFT) calculations predict a magnetic moment of  $\sim 1.8 \mu_B$  for the O<sub>2</sub> molecule when it is adsorbed on the surface of  $\alpha$ -alumina (0001)[45]. As mentioned earlier, physisorption of oxygen molecules at the  $V_S$  sites leading to the passivation of of these defects as donors has been demonstrated for these samples[20]. Therefore, it is reasonable to believe that O<sub>2</sub> molecules attached to the  $V_S$ -sites can act as spin-flip centres, which promote the inter valley (K-K') spin-flip scattering

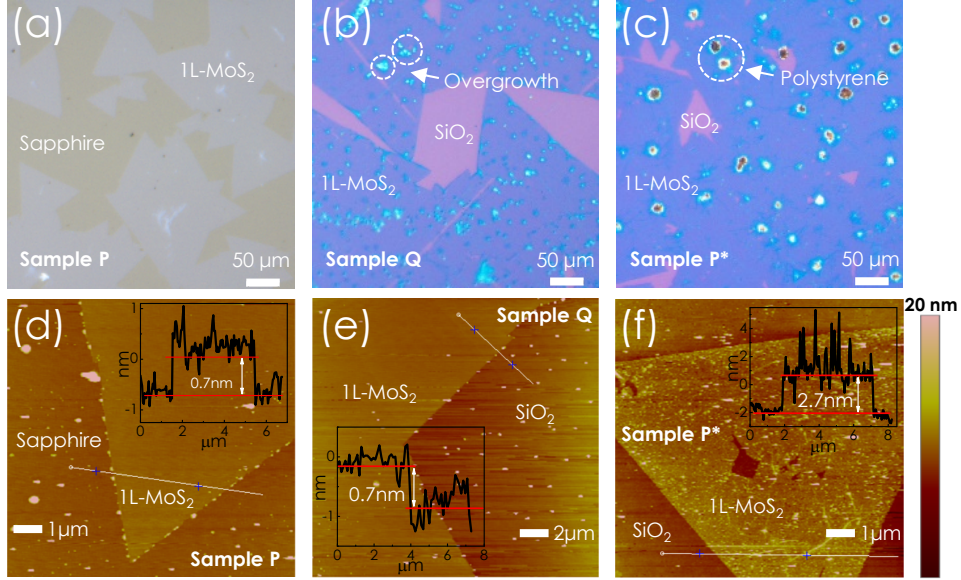


FIG. 5. Optical microscopic images of samples (a) P, (b) Q and (c) P\*. AFM topographic images of samples (d) P, (e) Q and (f) P\*. Insets of panels (d), (e), and (f) show the height distribution along the lines drawn across the boundaries of samples P, Q and P\*, respectively.

of the excitons/trions in MoS<sub>2</sub>. Note that the suppression of BL-intensity in the transferred sample (sample P\*) as compared to the 1L-MoS<sub>2</sub> film grown on sapphire substrate (sample P) as shown in Fig. 2 suggest a reduction of the density of the O<sub>2</sub> molecules adsorbed at the V<sub>S</sub>-sites. Like in case of SiO<sub>2</sub>/Si grown sample Q (see Fig. 4), removal of these molecules from the S-vacancy sites might also contribute to the recovery of  $|P|$  in transferred sample P\*.

It should be noted that after the suppression of the BL-intensity through annealing, if the as-grown samples P and Q are exposed to the ambient condition, the relative intensity of BL with respect to that of A exciton/trion feature has been found to return to its original value after several hours of exposure. This reversibility suggests that the air molecule are getting physically[20, 21] adsorbed and desorbed from the V<sub>S</sub>-sites in these films. However, similar experiment on the transferred sample P\* does not show much variation of BL-intensity even after keeping the sample in the ambient for several months as shown in supplementary figure S4. Note that the transfer process involves coating MoS<sub>2</sub> with polystyrene followed by baking at temperature comparable to that is used for vacuum annealing. It could be possible that the transfer process itself is facilitating the removal of

the adsorbed molecules from the  $V_S$ -sites and then provides an encapsulation of the layer that protects  $V_S$ -centres from air. Fig. 5(a-c) compare the optical microscopic images for samples P, Q and P\*. MoS<sub>2</sub> films covering large areas can be found for all the samples. Layer grown on sapphire substrate looks quite clean, whereas some small high contrast triangular overgrown structures can be seen on MoS<sub>2</sub> layer grown on SiO<sub>2</sub>/Si substrate. However, a much higher density of circular structures can be seen on transferred sample P\* [panel (c)]. These structures can be attributed to some bigger residues of polystyrene[34], which could not be dissolved completely in toluene at the final stage of the transfer process. Fig 5(d-f) show AFM micrographs for the three samples. Clear contrast between the MoS<sub>2</sub> flakes and the substrate is evident in these images. Average height of the flakes can be obtained from the line scan profiles recorded across the boundary between MoS<sub>2</sub> and the substrate at several places. Inset of each of the panels shows one such profile recorded along the white line shown in the image. For the samples P and Q, the average step height of the flakes has been found to be  $\sim 0.7$  nm. This ensures monolayer nature of the MoS<sub>2</sub> flakes in both the samples. Average roughness of these flakes is found to be  $\sim 0.12$  nm. In case of the transferred sample P\*, the average step height and the roughness of the flakes come out to be  $\sim 2.7$  nm and  $\sim 0.89$  nm, respectively. Both these values are clearly larger than those are obtained for the as grown samples P and Q, which clearly suggests that a thin capping layer still exists on MoS<sub>2</sub> in the transferred sample P\* even after cleaning the sample several times in toluene. All these findings strongly support our conjecture that the transfer process not only help in removing the physisorbed air molecules from MoS<sub>2</sub>, but also protect the layer from the ambient by introducing a coating on the surface.

In conclusion, vacuum annealing helps in removing air molecules from sulfur vacancy sites in the CVD grown 1L-MoS<sub>2</sub> that leads to the suppression of the broad luminescence (BL) feature that results from sulfur vacancy ( $V_S$ )-air-molecule defect complexes at low measurement temperatures. In case of sapphire grown 1L-MoS<sub>2</sub> sample, no difference between  $\sigma^-$  and  $\sigma^+$  polarized PL spectra could be found in the whole temperature range of investigation (85 to 300 K) when circularly polarized 633 nm laser light is used for excitation. Degree of circular polarization  $|P|$ , which has been defined as the ratio between the change in  $\sigma^-$  and  $\sigma^+$  polarized PL intensity and the overall PL intensity at a given photon energy, is found to be zero throughout the spectra even after the sample is vacuum annealed. On the other hand, in case of sample P\*, where 1L-MoS<sub>2</sub> layers grown on the sapphire substrate are

transferred on a SiO<sub>2</sub>/Si substrate,  $|P|$  at A-exciton/trion position is found to be as high as 0.8. This shows that the main cause for showing zero polarization at A-exciton/trion feature in case of the sapphire grown sample even after the annealing is likely to be the biaxial tensile strain, which is shown to be present in the as-grown layer. In case of the as-grown sample on SiO<sub>2</sub>/Si substrate,  $|P|$  is found to be zero over the entire photon energy range as well as the temperature range of investigation. However  $|P|$  at the A-exciton/trion position becomes as high as 0.25 after the vacuum annealing of the sample. This suggests that the recovery of polarization at the A-exciton/trion position upon annealing must be associated with the removal of air molecules from the  $V_S$  sites. The study thus shows that the strain as well as the physisorption of air molecules with  $V_S$  sites play key roles in governing the valley polarization property of CVD grown 1L-MoS<sub>2</sub>. It has also been found that the polystyrene assisted process adopted here for transferring CVD grown MoS<sub>2</sub> monolayers from sapphire substrates to SiO<sub>2</sub>/Si substrates not only facilitates the removal of physisorbed air molecules from the  $V_S$  sites but also shields the MoS<sub>2</sub> film from the environment by putting in place a long lasting capping layer. The transfer technique thus enhances the relative yield of A-exciton/trion transition by suppressing the BL transition. The method also significantly improves the valley polarization property of the film. Both the improvements are highly desirable for the development of valleytronic devices in the future.

**Acknowledgment:** We would like to acknowledge the financial support by Department of Science and Technology (DST) of Government of India (grant number: CRG/2018/001343). We are also thankful for various experimental opportunities provided by Industrial Research and Consultancy Centre (IRCC) and Sophisticated Analytical Instrument Facility (SAIF) of IIT Bombay. We sincerely thank Prof. Arindam Chowdhury for valuable discussions and help in doing certain experiments.

---

\* poulab007@gmail.com

- [1] Kin Fai Mak, Changgu Lee, James Hone, Jie Shan, and Tony F. Heinz. Atomically thin MoS<sub>2</sub> a new direct-gap semiconductor. *Phys. Rev. Lett.*, 105:136805, 2010.
- [2] Andrea Splendiani, Liang Sun, Yuanbo Zhang, Tianshu Li, Jonghwan Kim, Chi-Yung Chim, Giulia Galli, and Feng Wang. Emerging photoluminescence in monolayer MoS<sub>2</sub>. *Nano Lett.*,

- 10:1271, 2010.
- [3] Shinichiro Mouri, Yuhei Miyauchi, and Kazunari Matsuda. Tunable photoluminescence of monolayer MoS<sub>2</sub> via chemical doping. *Nano Lett.*, 13(12):5944–5948, 2013.
  - [4] Kin Fai Mak, Keliang He, Changgu Lee, Gwan Hyoung Lee, James Hone, Tony F Heinz, and Jie Shan. Tightly bound trions in monolayer MoS<sub>2</sub>. *Nature materials*, 12(3):207–211, 2013.
  - [5] Cong Mai, Andrew Barrette, Yifei Yu, Yuriy G Semenov, Ki Wook Kim, Linyou Cao, and Kenan Gundogdu. Many-body effects in valleytronics: direct measurement of valley lifetimes in single-layer MoS<sub>2</sub>. *Nano Lett.*, 14(1):202–206, 2014.
  - [6] Kin Fai Mak, Keliang He, Jie Shan, and Tony F Heinz. Control of valley polarization in monolayer MoS<sub>2</sub> by optical helicity. *Nature Nanotechnology*, 7(8):494–498, August 2012.
  - [7] Ting Cao, Gang Wang, Wenpeng Han, Huiqi Ye, Chuanrui Zhu, Junren Shi, Qian Niu, Pingheng Tan, Enge Wang, Baoli Liu, and Ji Feng. Valley-selective circular dichroism of monolayer molybdenum disulphide. *Nature Communications*, 3(1):887, June 2012.
  - [8] Hualing Zeng, Junfeng Dai, Wang Yao, Di Xiao, and Xiaodong Cui. Valley polarization in MoS<sub>2</sub> monolayers by optical pumping. *Nature Nanotechnology*, 7(8):490–493, August 2012.
  - [9] Di Xiao, Gui-Bin Liu, Wanxiang Feng, Xiaodong Xu, and Wang Yao. Coupled spin and valley physics in monolayers of MoS<sub>2</sub> and other group-VI dichalcogenides. *Phys. Rev. Lett.*, 108:196802, May 2012.
  - [10] Elizabeth J McCormick, Michael J Newburger, Yunqiu Kelly Luo, Kathleen M McCreary, Simranjeet Singh, Iwan B Martin, Edward J Cichewicz, Berend T Jonker, and Roland K Kawakami. Imaging spin dynamics in monolayer WS<sub>2</sub> by time-resolved kerr rotation microscopy. *2D Materials*, 5(1):011010, 2017.
  - [11] Prachi Budania, PT Baine, JH Montgomery, DW McNeill, SJN Mitchell, M Modreanu, and PK Hurley. Effect of post-exfoliation treatments on mechanically exfoliated MoS<sub>2</sub>. *Materials Research Express*, 4(2):025022, 2017.
  - [12] Gábor Zsolt Magda, János Pető, Gergely Dobrik, Chanyong Hwang, László P Biró, and Lev-ente Tapasztó. Exfoliation of large-area transition metal chalcogenide single layers. *Scientific reports*, 5(1):1–5, 2015.
  - [13] Seung Hyun Baek, Yura Choi, and Woong Choi. Large-area growth of uniform single-layer MoS<sub>2</sub> thin films by chemical vapor deposition. *Nanoscale research letters*, 10(1):1–6, 2015.
  - [14] P. K. Mohapatra, S. Deb, B. P. Singh, P. Vasa, and S. Dhar. Strictly monolayer large

- continuous MoS<sub>2</sub> films on diverse substrates and their luminescence properties. *Appl. Phys. Lett.*, 108:042101, 2016.
- [15] S. Deb, P. Chakrabarti, P. K. Mohapatra, B. K. Barick, and S. Dhar. Tailoring of defect luminescence in CVD grown monolayer MoS<sub>2</sub> film. *Appl. Surf. Sci.*, 445:542–547, 2018.
- [16] Alessandro Surrente, Dumitru Dumcenco, Zhuo Yang, Agnieszka Kuc, Yu Jing, Thomas Heine, Yen-Cheng Kung, Duncan K Maude, Andras Kis, and Paulina Plochocka. Defect healing and charge transfer-mediated valley polarization in MoS<sub>2</sub>/MoSe<sub>2</sub>/MoS<sub>2</sub> trilayer van der waals heterostructures. *Nano Lett.*, 17(7):4130–4136, 2017.
- [17] Sina Najmaei, Matin Amani, Matthew L Chin, Zheng Liu, A Glen Birdwell, Terrance P O’Regan, Pulickel M Ajayan, Madan Dubey, and Jun Lou. Electrical transport properties of polycrystalline monolayer molybdenum disulfide. *ACS nano*, 8(8):7930–7937, 2014.
- [18] Matin Amani, Matthew L Chin, Alexander L Mazzone, Robert A Burke, Sina Najmaei, Pulickel M Ajayan, Jun Lou, and Madan Dubey. Growth-substrate induced performance degradation in chemically synthesized monolayer MoS<sub>2</sub> field effect transistors. *Appl. Phys. Lett.*, 104(20):203506, 2014.
- [19] Vinod K Sangwan, Deep Jariwala, In Soo Kim, Kan-Sheng Chen, Tobin J Marks, Lincoln J Lauhon, and Mark C Hersam. Gate-tunable memristive phenomena mediated by grain boundaries in single-layer MoS<sub>2</sub>. *Nature nanotechnology*, 10(5):403–406, 2015.
- [20] S. Deb, P. Bhattacharyya, P. Chakrabarti, H. Chakraborti, K. Das Gupta, A. Sukla, and S. Dhar. Effect of oxygen adsorption on electrical and thermoelectrical properties of monolayer MoS<sub>2</sub>. *Phys. Rev. Applied*, 14:034030, 2020.
- [21] Sefaattin Tongay, Joonki Suh, Can Ataca, Wen Fan, Alexander Luce, Jeong Seuk Kang, Jonathan Liu, Changhyun Ko, Rajamani Raghunathanan, Jian Zhou, et al. Defects activated photoluminescence in two-dimensional semiconductors: interplay between bound, charged and free excitons. *Scientific reports*, 3(1):1–5, 2013.
- [22] Sefaattin Tongay, Jian Zhou, Can Ataca, Jonathan Liu, Jeong Seuk Kang, Tyler S. Matthews, Long You, Jingbo Li, Jeffrey C. Grossman, and Junqiao Wu. Broad-range modulation of light emission in two-dimensional semiconductors by molecular physisorption gating. *Nano Lett.*, 13:2831, 2013.
- [23] Haiyan Nan, Zilu Wang, Wenhui Wang, Zheng Liang, Yan Lu, Qian Chen, Daowei He, Pingheng Tan, Feng Miao, Xinran Wang, et al. Strong photoluminescence enhancement of



- MoS<sub>2</sub> through defect engineering and oxygen bonding. *ACS nano*, 8(6):5738–5745, 2014.
- [24] Philippe K Chow, Robin B Jacobs-Gedrim, Jian Gao, Toh-Ming Lu, Bin Yu, Humberto Terrones, and Nikhil Koratkar. Defect-induced photoluminescence in monolayer semiconducting transition metal dichalcogenides. *ACS nano*, 9(2):1520–1527, 2015.
- [25] C. R. Zhu, G. Wang, B. L. Liu, X. Marie, X. F. Qiao, X. Zhang, X. X. Wu, H. Fan, P. H. Tan, T. Amand, and B. Urbaszek. Strain tuning of optical emission energy and polarization in monolayer and bilayer MoS<sub>2</sub>. *Phys. Rev. B*, 88:121301, Sep 2013.
- [26] Hiram J Conley, Bin Wang, Jed I Ziegler, Richard F Haglund Jr, Sokrates T Pantelides, and Kirill I Bolotin. Bandgap engineering of strained monolayer and bilayer MoS<sub>2</sub>. *Nano Lett.*, 13(8):3626–3630, 2013.
- [27] Riccardo Frisenda, Matthias Drüppel, Robert Schmidt, Steffen Michaelis de Vasconcellos, David Perez de Lara, Rudolf Bratschitsch, Michael Rohlfing, and Andres Castellanos-Gomez. Biaxial strain tuning of the optical properties of single-layer transition metal dichalcogenides. *npj 2D Materials and Applications*, 1(1):1–7, 2017.
- [28] Amber McCreary, Rudresh Ghosh, Matin Amani, Jin Wang, Karel-Alexander N Duerloo, Ankit Sharma, Karalee Jarvis, Evan J Reed, Avinash M Dongare, Sanjay K Banerjee, et al. Effects of uniaxial and biaxial strain on few-layered terrace structures of MoS<sub>2</sub> grown by vapor transport. *ACS nano*, 10(3):3186–3197, 2016.
- [29] Pranjal Kumar Gogoi, Zhenliang Hu, Qixing Wang, Alexandra Carvalho, Daniel Schmidt, Xinmao Yin, Yung-Huang Chang, Lain-Jong Li, Chornng Haur Sow, A. H. Castro Neto, Mark B. H. Breese, Andriwo Rusydi, and Andrew T. S. Wee. Oxygen passivation mediated tunability of trion and excitons in MoS<sub>2</sub>. *Phys. Rev. Lett.*, 119:077402, 2017.
- [30] Linfeng Sun, Xiaoming Zhang, Fucui Liu, Youde Shen, Xiaofeng Fan, Shoujun Zheng, John TL Thong, Zheng Liu, Shengyuan A Yang, and Hui Ying Yang. Vacuum level dependent photoluminescence in chemical vapor deposition-grown monolayer MoS<sub>2</sub>. *Scientific reports*, 7(1):1–9, 2017.
- [31] Rahul Rao, Victor Carozo, Yuanxi Wang, Ahmad E Islam, Nestor Perea-Lopez, Kazunori Fujisawa, Vincent H Crespi, Mauricio Terrones, and Benji Maruyama. Dynamics of cleaning, passivating and doping monolayer MoS<sub>2</sub> by controlled laser irradiation. *2D Materials*, 6:045031, 2019.
- [32] Nihit Saigal, Isabelle Wielert, Davor Čapeta, Nataša Vujičić, Boris V. Senkovskiy, Martin

- Hell, Marko Kralj, and Alexander Grüneis. Effect of lithium doping on the optical properties of monolayer MoS<sub>2</sub>. *Appl. Phys. Lett.*, 112:121902, 2018.
- [33] Nihit Saigal and Sandip Ghosh. Evidence for two distinct defect related luminescence features in monolayer MoS<sub>2</sub>. *Appl. Phys. Lett.*, 109:122105, 2016.
- [34] Alper Gurarlsan, Yifei Yu, Liqin Su, Yiling Yu, Francisco Suarez, Shanshan Yao, Yong Zhu, Mehmet Ozturk, Yong Zhang, and Linyou Cao. Surface-energy-assisted perfect transfer of centimeter-scale monolayer and few-layer MoS<sub>2</sub> films onto arbitrary substrates. *ACS Nano*, 8(11):11522–11528, 2014.
- [35] Pranab K Mohapatra, Kamalakannan Ranganathan, and Ariel Ismach. Selective area growth and transfer of high optical quality MoS<sub>2</sub> layers. *Advanced Materials Interfaces*, 7(24):2001549, 2020.
- [36] Hong Li, Qing Zhang, Chin Chong Ray Yap, Beng Kang Tay, Teo Hang Tong Edwin, Aurelien Olivier, and Dominique Baillargeat. From bulk to monolayer MoS<sub>2</sub>: evolution of raman scattering. *Advanced Functional Materials*, 22(7):1385–1390, 2012.
- [37] Biswanath Chakraborty, Achintya Bera, D. V. S. Muthu, Somnath Bhowmick, U. V. Waghmare, and A. K Sood. Symmetry-dependent phonon renormalization in monolayer MoS<sub>2</sub> transistor. *Phys. Rev. B*, 85:161403(R), 2012.
- [38] John E Ayers, Tedi Kujofsa, Paul Rago, and Johanna Raphael. *Heteroepitaxy of semiconductors: theory, growth, and characterization*. 2nd edn (CRC press), 2016.
- [39] Hui Ye and Jinzhong Yu. Germanium epitaxy on silicon. *Science and Technology of Advanced Materials*, 2014.
- [40] Dumitru Dumcenco, Dmitry Ovchinnikov, Kolyo Marinov, Predrag Lazic, Marco Gibertini, Nicola Marzari, Oriol Lopez Sanchez, Yen-Cheng Kung, Daria Krasnozhon, Ming-Wei Chen, et al. Large-area epitaxial monolayer MoS<sub>2</sub>. *ACS nano*, 9(4):4611–4620, 2015.
- [41] Tao Yu and MW Wu. Valley depolarization due to intervalley and intravalley electron-hole exchange interactions in monolayer MoS<sub>2</sub>. *Phys. Rev. B*, 89(20):205303, 2014.
- [42] Eito Asakura, Masaki Suzuki, Shutaro Karube, Junsaku Nitta, Kosuke Nagashio, and Makoto Kohda. Detection of both optical polarization and coherence transfers to excitonic valley states in cvd-grown monolayer MoS<sub>2</sub>. *Applied Physics Express*, 12(6):063005, 2019.
- [43] Emilio Scalise, Michel Houssa, G Pourtois, VV Afanas, Andre Stesmans, et al. First-principles study of strained 2d MoS<sub>2</sub>. *Physica E: Low-dimensional Systems and Nanostructures*, 56:416–

421, 2014.

- [44] Linus Pauling. *The nature of the chemical bond: and the structure of molecules and crystals: an introduction to modern structural chemistry*. Cornell University Press, Ithaca, 1960.
- [45] Hui Wang, Chuntai Shi, Jun Hu, Sungho Han, C Yu Clare, and RQ Wu. Candidate source of flux noise in squids: adsorbed oxygen molecules. *Phys. Rev. Lett.*, 115(7):077002, 2015.

# Supplementary Information

## **Effect of strain and sulfur vacancies on the luminescence and valley polarization properties of CVD grown monolayer MoS<sub>2</sub> films**

Poulab Chakrabarti\*, Faiha Mujeeb, Subhabrata Dhar

Department of Physics, Indian Institute of Technology Bombay, Mumbai-400076, India

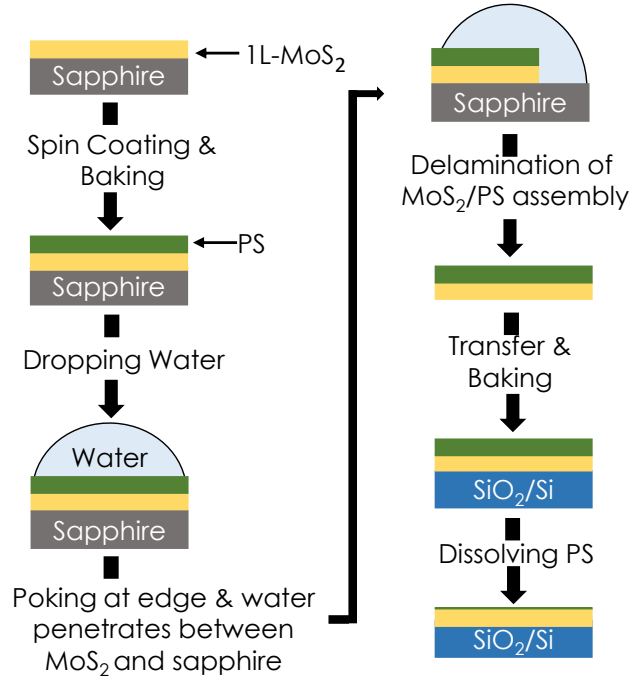


FIG. 6. The surface-energy assisted transfer process[34, 35] of 1L-MoS<sub>2</sub> is schematically shown. Here, Polystyrene (PS) was used as the carrier polymer and its solution was prepared by dissolving 9 g of PS with a molecular weight of 280,000 g/mol in 100 ml of toluene. The solution was then spin-coated (500 rpm for 30 s and 3500 rpm for 60 s) on 1L-MoS<sub>2</sub> grown on sapphire and baked at 80-90 °C for 35 minutes and 120 °C for 10 minutes, successively. Then a water droplet was dropped onto the PS layer. Water has a natural tendency to penetrate between the MoS<sub>2</sub> film and the substrate due to the differences in their surface energies, but the penetration actually cannot start by itself. Gentle poking at the edge of the MoS<sub>2</sub>/PS assembly was required to initiate the water penetration underneath MoS<sub>2</sub> layer. As a result, the MoS<sub>2</sub>/PS assembly got lifted and it was transferred onto SiO<sub>2</sub>/Si substrate. After that, it had to be baked for 80-90 °C for 35 minutes and 120 °C for 10 minutes. Finally, the PS layer was removed by several times rinsing it in toluene.

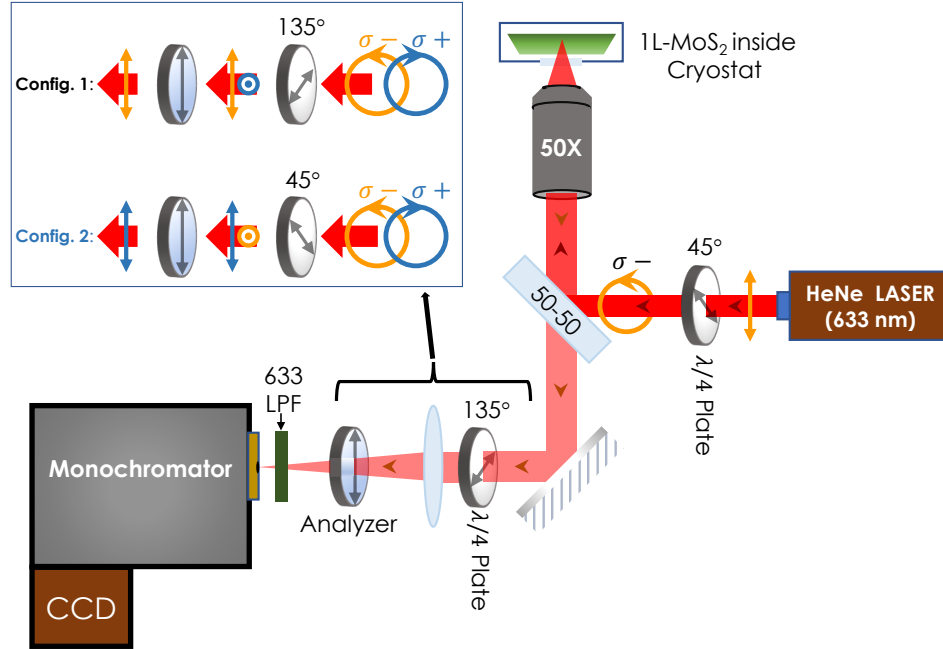


FIG. 7. Schematic depiction of the circular polarization selective micro photoluminescence (PL) setup. The sample was kept inside a pour-fill type liquid nitrogen cryostat under high vacuum at  $\sim 10^{-6}$  mbar pressure where the sample temperature can be varied from 85 K to 400 K. A linearly polarized Helium Neon (HeNe, 633 nm) laser is made left circularly polarized ( $\sigma^-$ ) by a  $45^\circ$  oriented achromatic quarter waveplate and used as the excitation source. The beam was then focused on the sample through a quartz glass window, using a  $50\times$  long working distance objective of 0.5 numerical aperture (NA). The collection of backscattered PL signal was also done by the same objective lens and it was further passed through another quarter waveplate and a Glan-Taylor analyzer placed in front of the entrance slit of the monochromator. As shown in the inset of this figure, the quarter waveplate is rotated by  $90^\circ$  to selectively choose  $\sigma^-$  (config. 1) and  $\sigma^+$  (config. 2) photons which is detected by a Peltier cooled CCD attached to the 0.55 m focal length monochromator. A 633 nm long pass filter (LPF) is placed in front of the monochromator entrance to block the elastically scattered laser light. The same setup is used for Raman spectroscopy, where the HeNe laser and the 633 nm LPF are replaced by a 532 nm diode pumped solid state (DPSS) laser and a Raman compatible ultra sharp 532 nm long pass filter, respectively.

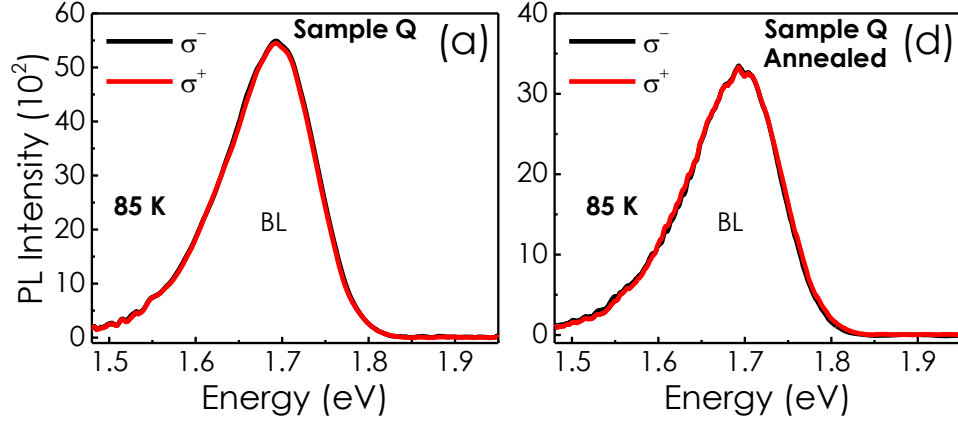


FIG. 8. Circular polarization resolved PL spectra for as-grown MoS<sub>2</sub> on SiO<sub>2</sub>/Si (sample Q) recorded at 85 K (a) before and (b) after annealing, where left circularly polarized ( $\sigma^-$ ) 633 nm laser is used for excitation. In both the cases, A-exciton/trion feature is absent and the spectra are dominated only by the  $V_S$  related BL peak. As discussed in the main text, here also, BL feature does not show any polarization contrast before and after annealing. The absence of A-exciton/trion feature can be attributed to the low excitation power and energy of the 633 nm laser[21], at which the radiative recombination rate of the free excitons is overwhelmed by that of the excitons captured at the  $V_S$ -sites at low temperatures.

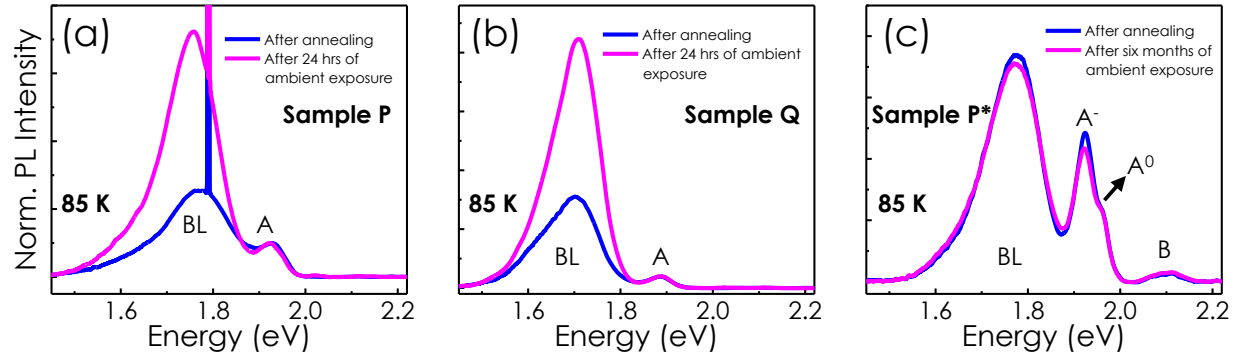


FIG. 9. Blue curves in panel (a), (b) and (c) show normalized (at  $A^0$  peak) PL spectra at 85 K for samples P, Q and P\*, respectively, recorded after annealing at 400 K temperature for 30 minutes in high vacuum ( $\sim 10^{-6}$  mbar) condition. After that, the vacuum was broken at room temperature and all the samples were exposed to ambient condition for 24 hours. Again as grown sample P and Q were taken down to 85 K temperature and the normalized (at  $A^0$ ) PL spectra for these samples are plotted in magenta color in panel (a) and (b) respectively. It can be seen that the intensity of BL feature with respect to that of  $A^0$  peak has increased and returned to its pre-annealed value (see figure 2 of main text) for sample P and Q. Interestingly for transferred sample P\*, the intensity of BL feature relative to  $A^0$  peak remains constant after 24 hours exposure of the sample in ambience. Finally, the transferred sample P\* was kept in ambient condition for 6 months. The magenta curve in panel (c) is showing the low temperature (85 K) normalized (at  $A^0$ ) PL spectrum of sample P\* after 6 month of ambient exposure and it can be seen that it has hardly changed. So, the polystyrene coating gives a long lasting protection to the sample from air.